Desiccant Enhanced Evaporative Air Conditioning: Parametric Analysis and Design

Preprint

J. Woods and E. Kozubal

NOTICE

Available electronically at http://www.osti.gov/bridge

Available for a processing fee to U.S. Department of Energy
and its contractors, in paper, from:

> U.S. Department of Energy
> Office of Scientific and Technical Information
> P.O. Box 62
> Oak Ridge, TN 37831-0062
> phone: 865.576.8401
> fax: 865.576.5728
> email: mailto:reports@adonis.osti.gov

Available for sale to the public, in paper, from:

> U.S. Department of Commerce
> National Technical Information Service
> 5285 Port Royal Road
> Springfield, VA 22161
> phone: 800.553.6847
> fax: 703.605.6900
> email: orders@ntis.fedworld.gov
> online ordering: http://www.ntis.gov/help/ordermethods.aspx

Cover Photos: (left to right) PIX 16416, PIX 17423, PIX 16560, PIX 17613, PIX 17436, PIX 17721

Printed on paper containing at least 50% wastepaper, including 10% post consumer waste.

Topic 8. Advanced or innovative HVAC&R systems and system components

Desiccant Enhanced Evaporative Air Conditioning: Parametric Analysis and Design

Jason Woods[*] and Eric Kozubal

National Renewable Energy Laboratory, Golden, Colorado, USA

[*]Corresponding email: jason.woods@nrel.gov

SUMMARY

This paper presents a parametric analysis using a numerical model of a new concept in desiccant and evaporative air conditioning. The concept consists of two stages: a liquid desiccant dehumidifier and a dew-point evaporative cooler. Each stage consists of stacked air channel pairs separated by a plastic sheet. In the first stage, a liquid desiccant film removes moisture from the process (supply-side) air through a membrane. An evaporatively-cooled exhaust airstream on the other side of the plastic sheet cools the desiccant. The second-stage indirect evaporative cooler sensibly cools the dried process air. We analyze the tradeoff between device size and energy efficiency. This tradeoff depends strongly on process air channel thicknesses, the ratio of first-stage to second-stage area, and the second-stage exhaust air flow rate. A sensitivity analysis reiterates the importance of the process air boundary layers and suggests a need for increasing airside heat and mass transfer enhancements.

INTRODUCTION

Liquid desiccants (LDs), or hygroscopic salt solutions, are used in air conditioners (a/c) to absorb water vapor from the air. They are reconcentrated with heat in a regenerator, enabling them to reabsorb moisture. A LD can dehumidify air below 20% relative humidity, offering cooling techniques that are adaptive to sensible and latent loads when combined with an indirect evaporative cooler (IEC). Kozubal et al. (2011) presented a new desiccant enhanced evaporative (DEVAP) a/c that combines an evaporatively-cooled LD dehumidifier with a dew-point IEC. For commercial buildings, they showed 40-80% energy savings and an 80% peak electric demand reduction compared to efficient vapor compression a/c (Kozubal et al. 2011). A numerical model of this process was validated with prototype testing (Woods and Kozubal 2012) for a range of flow rates, LD concentrations, and psychrometric conditions.

The concept consists of two stages of arrays of channel pairs (refer to Figure 1). In the first stage, a mixture of outdoor air and return air (state 1) enters the supply-side channels (s1), and outdoor air (3) enters the exhaust-side channels (e1). The supply-side channels are lined with LD films contained behind hydrophobic, microporous membranes. The LD films are gravity driven, after being pumped to the top of the device. The LD absorbs moisture from the mixed-air stream, converting the latent energy in the air to sensible energy. This energy moves across a plastic sheet and drives evaporation of water into airstream e1, which exits as humid exhaust air (4). Airstream s1 becomes s2 in the second stage, where it is cooled by water evaporating into a separate exhaust airstream (e2) in counterflow. Airstream e2 is siphoned off from the cool-dry supply air (2). It matches the ventilation air brought in with the mixed air, and thus the ratio of airstream e2 to the mixed air flow rate (EAF_2) is equal to the outdoor air fraction. In both stages, the water is sprayed onto wicked surfaces in channels e1 and e2.

The purpose of this research is to determine the key design parameters for a DEVAP a/c. We do this by first developing a design method based on the tradeoff between the device size (a surrogate for cost) and

energy efficiency. We then determine the sensitivity of the size and efficiency to each transport resistance and design parameter. This shows which resistances in the numerical model need to be accurately predicted and where future research should focus to improve efficiency and reduce size and cost.
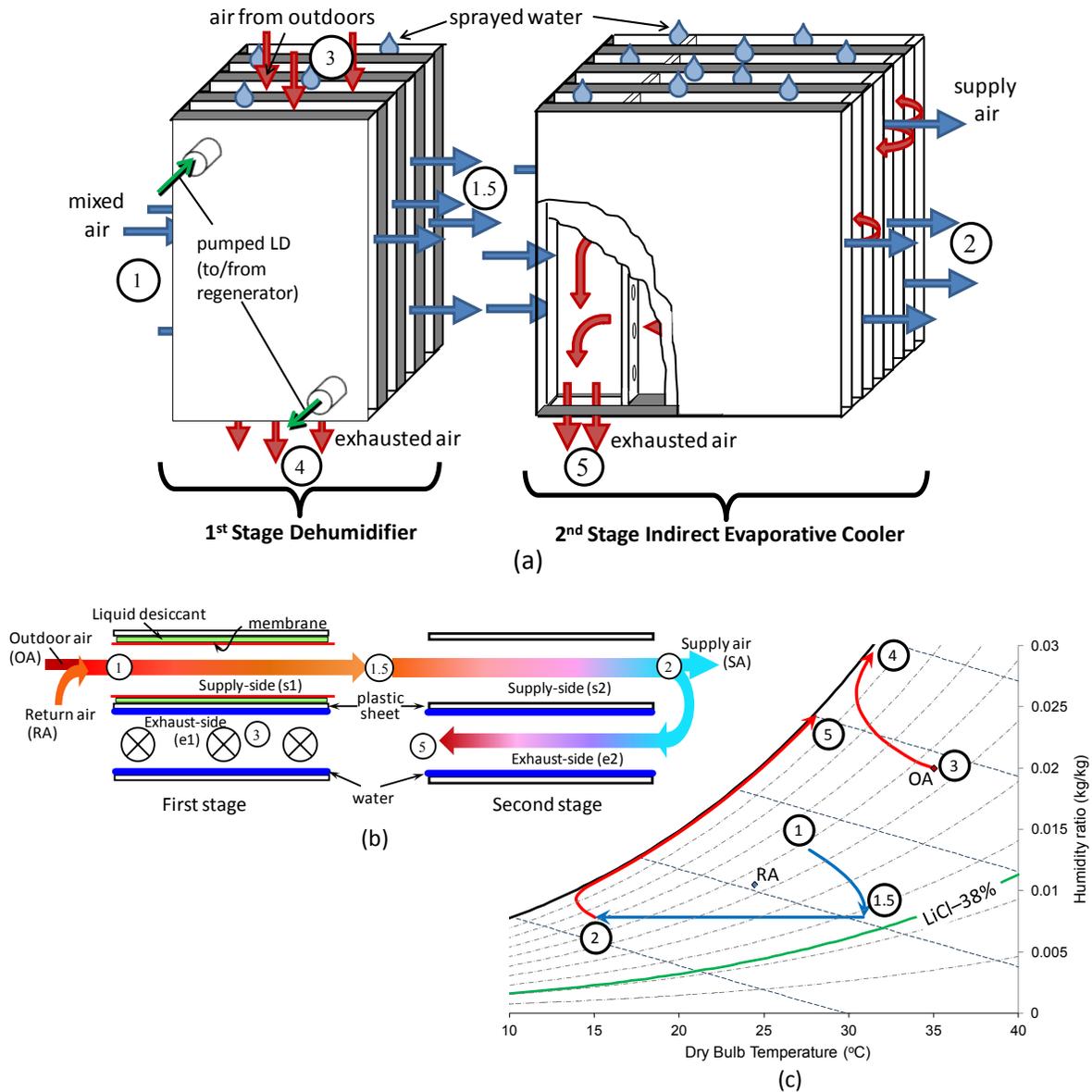
Figure 1: (a) Schematic of DEVAP a/c, (b) top view of channel pair, and (c) air states on a psychrometric chart. LiCl-38% is humidity ratio in equilibrium with 38% concentration LiCl.

METHODS

We use our recently validated numerical model (Woods and Kozubal 2012) to examine the key design parameters for a DEVAP a/c. This section develops a design tool based on the tradeoff between initial size and energy efficiency, and then describes the sensitivity and parametric analyses that are used to determine the importance of the design parameters.

Design tradeoff

Determining the cost-optimal design of a DEVAP a/c requires estimates of manufacturing cost and simulations of cooling load profiles in different climates, which are beyond the scope of this paper. Instead, we search for near optimal designs by plotting the specific surface area, $A_{specific}$ (m²/kW) versus the coefficient of performance, *COP*, at a single worst-case design condition (outdoor air: 35°C dry bulb, 27°C wet bulb; return air: 24.5°C dry bulb, 18°C wet bulb). In general, reducing $A_{specific}$ results in a lower *COP*. When plotted against each other, near-optimal designs will be at the corner of high *COP* and low $A_{specific}$. The specific surface area is the surface area of the device available for heat and mass transfer (*A*) divided by the total space cooling rate:

$$A_{specific} = \frac{A}{\dot{m}_{SA}\Delta h} \tag{1}$$

where $\dot{m}_{SA}$ is the supply air mass flow rate and Δh the specific enthalpy change from return air to the supply air (ventilation is not included). The source *COP* is:

$$COP_{source} = \frac{\dot{m}_{SA}\Delta h}{\left(W_{elec}3.4 + Q_{th}1.1\right)} \tag{2}$$

where W_{elec} and Q_{th} are the electric and thermal energy inputs, and the 3.4 and 1.1 are the site-to-source energy factors for grid-provided electricity and natural gas (Deru and Torcellini 2007). These values also approximate the relative costs of electricity and natural gas. Electricity is required for the fans (pump electricity is negligible) and is calculated with pressure drop for fully developed laminar flow through parallel plate channels and an assumed fan efficiency of 0.5 for a variable-speed plenum fan (see e.g. Fox et al. 2004). Thermal energy from burning natural gas is required for the regenerator and is calculated as:

$$Q_{th} = \eta_{regen}\dot{m}_{MA}\Delta\omega_{MA}h_{fg} \tag{3}$$

where $\dot{m}_{MA}$ and $\Delta\omega_{MA}$ are the mixed-air mass flow rate and change in the mixed-air humidity ratio, and h_{fg} the enthalpy of vaporization of water. Demonstrated regenerator efficiencies (η_{regen}) are 0.6-0.8 for single effect (Yin and Zhang 2010) and 1.05 for 1.5-effect (Lowenstein 2005). This paper focuses only on the DEVAP conditioner component, and assumes a constant regenerator efficiency of 1.0, as well as a constant inlet LD concentration of 0.40, and an outlet of 0.38. The LD used in the model is lithium chloride (LiCl).

Sensitivity and parametric analyses

This section describes the sensitivity and parametric analyses used to find the key design parameters. The sensitivity analysis determines the importance of each heat and mass transfer resistance between the supply and exhaust airstreams, which will help focus future redesigns on large-impact changes. It is performed around a design similar to the previous prototype (Woods and Kozubal 2012), and for a sensible heat ratio (*SHR*) of 0.6 and a specific enthalpy from the return air to the supply air (Δh) of 16 kJ/kg. A sensitivity index is calculated for each transport resistance, x_i, based on the percentage of uncertainty from that resistance:

$$S_{A-x_i} = \left(\frac{\partial A_{specific}}{\partial x_i}x_i\right)^2 \Big/ \sum_{x_i}\left(\frac{\partial A_{specific}}{\partial x_i}x_i\right)^2 \tag{4}$$

3

The parametric analysis considers *SHR*s of 0.5, 0.6, and 0.7 (Table 1). Some design parameters are fixed. The LD parameters are fixed to remove regenerator effects. The tradeoff between *COP* and $A_{specific}$ is small for the other fixed parameters. The varied parameters are randomly selected from a uniform distribution over the range shown in Table 1. Simulations calculate $A_{specific}$ and *COP* (Table 2) for 2000 combinations of independent variables for each *SHR*. Two other dependent variables of interest are Δh, which is the cooling rate per unit of air delivered, and EAF_2, which floats to meet the *SHR*. In real installations, EAF_2 is a design variable that is controlled to meet the *SHR*.

The values of $A_{specific}$ and *COP* are plotted against each other to find the near-optimal designs (points with the highest *COP* at each $A_{specific}$). The correlation between the independent and dependent variables just for the designs on the optimal line are shown on a correlogram plot (Figure 3) created with the program *R* (R 2011). This plot shows how each of these parameter affects $A_{specific}$ and *COP*, the values and trends of the design variables giving the optimal design line, and the relationships between these variables along this optimal line.

Table 1. Independent variables (EAF=exhaust air fraction, st1=first stage, st2=second stage, MA=mixed air, OA=outdoor air, RA=return air, D=mass diffusivity, k=thermal conductivity)

Design constraints (fixed)			Transport coefficients (fixed)		
OA temperature	T_{OA}	35°C	Membrane (mass)	$(D/d)_{mem}$	0.2 m/s
OA wet-bulb	$T_{wb,OA}$	27°C	Membrane (heat)	$(k/d)_{mem}$	950 W/m²K
RA temperature	T_{RA}	24.5°C	Plate	$(k/d)_{plate}$	300 W/m²K
RA wet-bulb	$T_{wb,RA}$	18°C	LD film thickness	d_{LD}	0.5 mm
Sensible heat ratio	*SHR*	0.5, 0.6, 0.7	Water film thickness	d_{water}	0.5 mm

Design variables (fixed)			Design variables (set within range)		
MA flow rate	$\dot{m}_{MA}$	0.2 kg/s	st1 exhaust (EAF_1)	$\dot{m}_{e1}/\dot{m}_{MA}$	0.4-0.8
st1 length	L_1	0.15 m	Total area	A	20-150 m²
st1 width	W_1	0.5 m	st1 area ratio ($A_{1\text{-}ratio}$)	A_1/A	0.10-0.35
st2 length	L_2	0.35 m	st1 supply-channel gap	H_{s1}	1-3 mm
st2 width	W_2	0.5 m	st1 exh-channel gap	H_{e1}	1-3 mm
LD concentration	C_{LD}	0.4	st2 supply-channel gap	H_{s2}	1-3 mm
LD conc. change	ΔC_{LD}	-0.02	st2 exh-channel gap	H_{e2}	1-3 mm

Table 2. Dependent variables

Design variables (calculated)	
st2 exhaust (EAF_2)	$\dot{m}_{e2}/\dot{m}_{MA}$
Performance metrics	
Specific enthalpy change (kJ/kg)	Δh
Coefficient of performance	*COP*
Total specific surface area (m²/kW)	$A_{specific}$

RESULTS

Sensitivity analysis: transport resistances

Table 3 shows the sensitivity of $A_{specific}$ to each transport resistance using Eq. (4). Mass transfer, particularly the mixed-air boundary layer, controls the first-stage specific area. Heat transfer also mainly the mixed-air boundary layer, controls the second-stage area. Thus, reducing the air-side resistances could significantly reduce the required area and device size.

Table 3: Sensitivity of $A_{specific}$ to each transport coefficient

Resistance:	Stage 1		Stage 2	
	Mass transfer	Heat transfer	Mass transfer	Heat transfer
Mixed air	79.0%	0.1%	n/a	92.6%
Membrane	6.4%	0.0%	n/a	n/a
Liquid desiccant	12.1%	0.4%	n/a	n/a
Plate	n/a	0.5%	n/a	2.3%
Water	n/a	0.4%	n/a	0.4%
Exhaust air	1.1%	0.0%	4.3%	0.5%
Total	98.6%	1.4%	4.3%	95.7%

Parametric analysis: design parameters

This section presents the parametric analysis results, which show the effects of the design parameters on device size and *COP*. Figure 2 shows $A_{specific}$ and *COP* for each random set of design parameters for the three values of *SHR*. The *optimal design line* is indicated with the dashed line. A tradeoff is clearly seen between size and efficiency. To the left are small, inefficient designs and to the right are large, efficient designs. The bottom right plot in Figure 2 shows the optimal lines for each *SHR*. Higher *SHR* requires more area for a given *COP*. This indicates the importance of the second-stage area, which is proportional to SHR.

Figure 3 looks *only* at the designs on the optimal design line. It plots each set of independent and dependent variables associated with these optimal designs against one another (upper right). The variables are listed along the diagonal, and their minimum and maximum values are shown along the top and the right side. In the lower left, positive correlations are indicated with a clockwise blue pie, and negative correlations with a counterclockwise red pie. The magnitudes of the correlations are indicated by the size and darkness of the shaded pies.
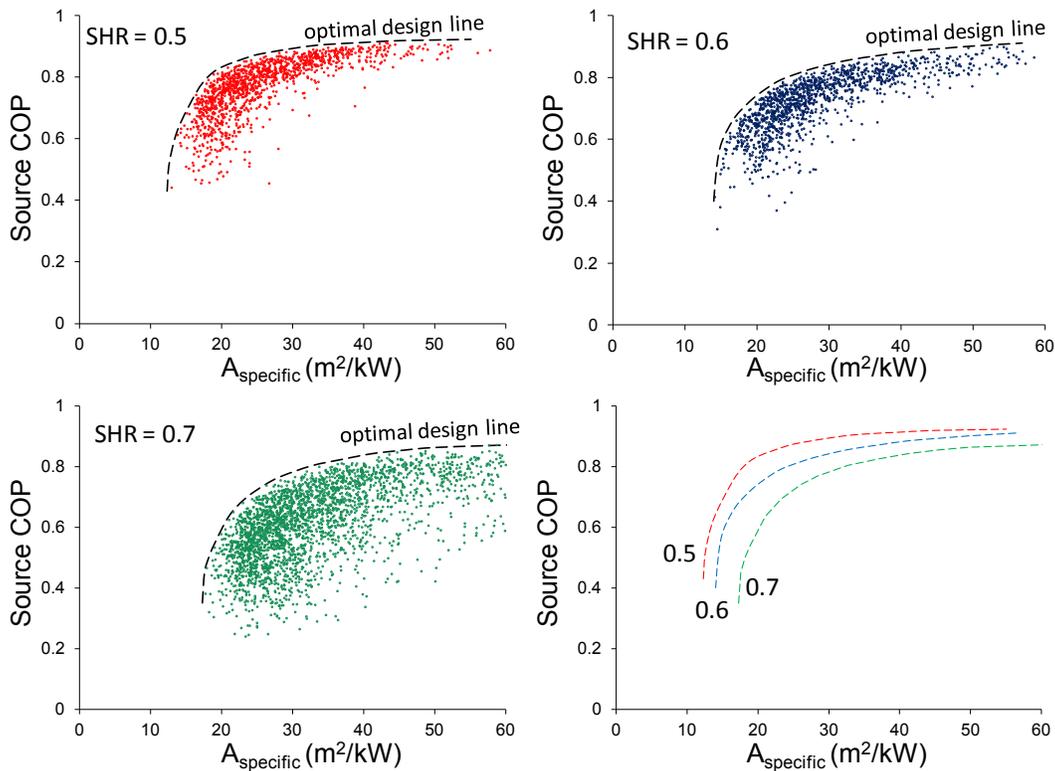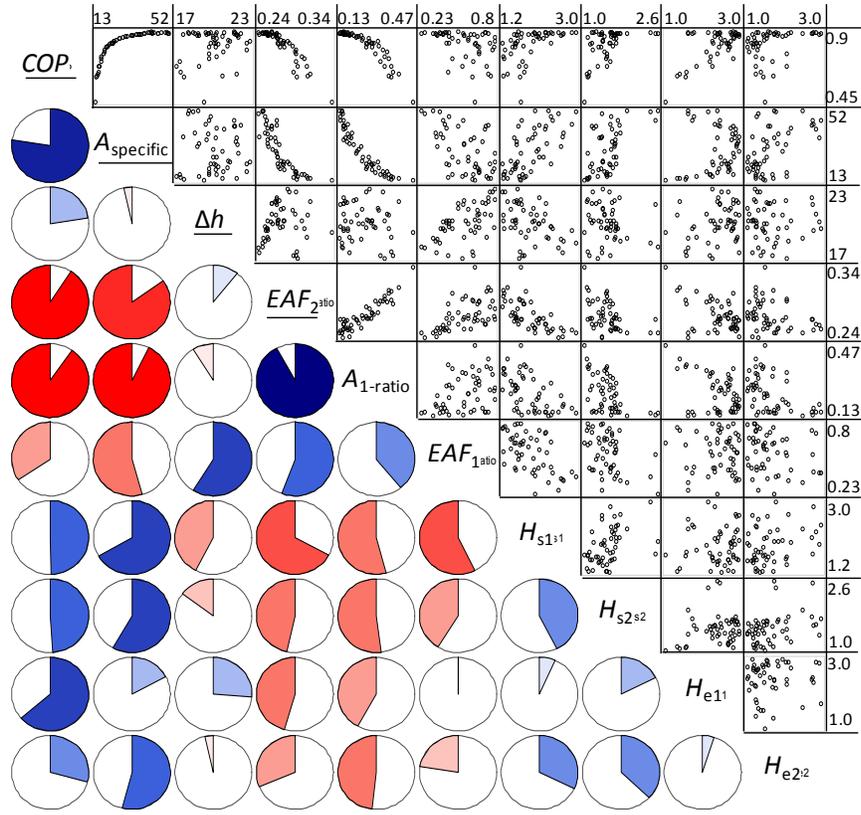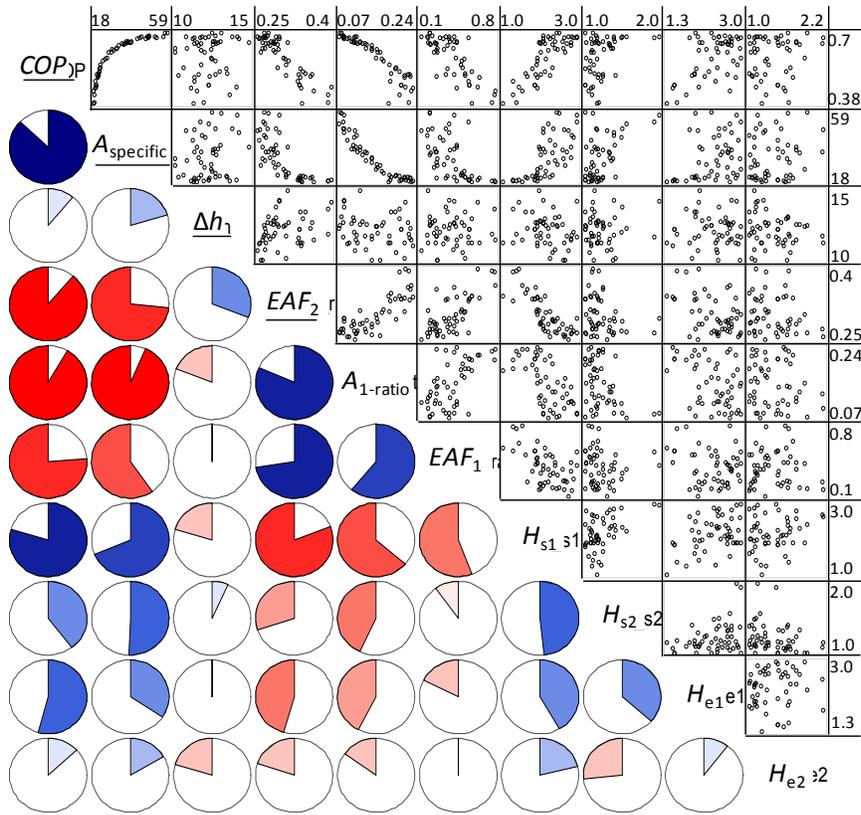

Figure 2: Source COP and specific area of each parametric analysis run. The bottom right plot shows the optimal design line for each SHR.

5

(a)

(b)

Figure 3: Correlogram for (a) SHR=0.5, (b) SHR=0.7. Dependent variables _underlined_.

There are several points to make from Figure 3, which relate to the *SHR*, the key design variable tradeoff between $A_{1\text{-}ratio}$ and EAF_2, and the channel thicknesses.

<u>SHR</u>: There are three reasons for the difference between the optimal lines of *SHR*=0.5 and *SHR*=0.7 in Figure 2, which can be seen by referring to Figure 3. First, more second-stage area is required for *SHR*=0.7 (0.07<$A_{1\text{-}ratio}$<0.24) than for SHR=0.5 (0.13<$A_{1\text{-}ratio}$<0.47). Second, the higher EAF_2 required for *SHR*=0.7 means more regeneration energy (Eq. (3)) is needed for a given cooling rate because more of this dehumidified air is being exhausted with exhaust airstream 2-5. This results in a lower *COP*. Third, Δh is lower for *SHR*=0.7, which means a higher flow rate and more fan power per kW of cooling. This also lowers *COP*.

<u>Design tradeoff</u>: There is a strong positive correlation between $A_{1\text{-}ratio}$ and EAF_2. Each of these design variable has a strong negative correlation with *COP* and with A_{specific}. In other words, increasing either $A_{1\text{-}ratio}$ or EAF_2 will reduce A_{specific} (good), but also reduce *COP* (bad). These two variables are also tied to the *SHR*, with higher $A_{1\text{-}ratio}$ (more first-stage dehumidification) requiring higher EAF_2 (more second-stage sensible cooling) for a given *SHR*.

<u>Air channel thicknesses</u>: The channel thicknesses have a positive correlation with *COP* and A_{specific}. Reducing channel size will reduce the required area, but also increase the fan power and therefore reduce *COP*. Consistent with the sensitivity analysis results, the supply-side air channels (H_{s1} and H_{s2}) are more important than the exhaust channels in reducing the area. The scatter plots for H_{s2} in Figure 3 indicate that optimal designs require small channels. These smaller channels increase the heat transfer coefficients and reduce the required second-stage area (and therefore A_{specific}). This effect on A_{specific} is larger than on *COP*, so most points on the optimal design line are for small H_{s2}. Alternatively, the first-stage exhaust (H_{e1}) has a stronger correlation with *COP* than with A_{specific}, so larger channel thicknesses are preferred.

DISCUSSION

The range of *COP*s presented in the figures deserves further explanation. The *COP* is near that of a vapor compression a/c, implying little energy savings. However, the plotted *COP*s are for worst-case design conditions, and the *COP* of a DEVAP a/c increases dramatically for less humid outdoor conditions when evaporative cooling is leveraged. A vapor compression a/c uses nearly the same power per kW of cooling regardless of humidity. As mentioned in the Introduction, building energy simulations (Kozubal et al. 2011) have shown 40-80% energy savings over vapor compression a/c in various U.S. climates.

The size and cost of a DEVAP a/c must be competitive with a vapor compression a/c to achieve market penetration. Like a vapor compression a/c, the tradeoff between size and efficiency is inherent to designing a DEVAP a/c. This work shows that the design depends on the application, particularly through the *SHR*. However, two key trends consistent across *SHR* are the channel sizes and the tradeoff between $A_{1\text{-}ratio}$ and EAF_2.

For a fixed first-stage area, EAF_2 controls the *SHR*. TO achieve a certain SHR, a design with a large first stage requires a high EAF_2, while a design with a large second stage requires a lower EAF_2. The former results in low *COP*s, while the latter results in a larger device (high A_{specific}). The former is preferred if the low *COP*s are seen only at peak loads, which occur during a small part of the cooling season. A controller is then required to maintain high *COP* during non-peak loads by minimizing EAF_2, with C_{LD}, and EAF_1 also being used to control *SHR*. The complexity of these advanced controllers is unknown at this time.

This controllability is a significant advantage of a DEVAP a/c, which can provide *SHR* ranging from $-\infty$ (adiabatic dehumidification) to 1 (indirect evaporate cooling). A vapor compression a/c typically provides an *SHR* near 0.7 to 0.8, and usually relies on reheating the air after dehumidification to achieve a low *SHR*. For details about this controllability, see Kozubal et al. (2011) and Woods and Kozubal (2012).

This analysis assumes laminar flow and indicates that small channel sizes, particularly on the supply side, are required to decrease size and cost. Small channels (< 1mm) can be difficult to manufacture. Alternatively, unsteady or turbulent flow can enhance heat and mass transfer in larger channels, which provides the same benefit as smaller channels with laminar flow.

CONCLUSIONS

This paper presents a design tool along with sensitivity and parametric analyses for an evaporatively cooled LD a/c. The study concluded that:

- There is an inherent design tradeoff between *COP* and size.
- $A_{1\text{-}ratio}$ and EAF_2 show strong correlations with *COP* and size. Once designed, a device's first-stage area is fixed, but EAF_2 is not. Controlling EAF_2, along with other parameters, sets the *SHR*. It will be important to minimize EAF_2, which has a strong negative correlation with *COP*, during off-peak times by controlling other parameters (e.g., C_{LD}).
- The key transport resistances in this new concept are the mass transfer resistance of the supply-side air in the first stage and the heat transfer resistance of the supply-side air in the second stage. This points to a need for either (1) structural channels that can maintain consistent, narrow dimensions, or (2) larger, more easily manufactured channels with enhancements that increase heat and mass transfer compared to laminar flow.

ACKNOWLEDGEMENT

REFERENCES

Deru, M. and P. Torcellini 2007. Source Energy and Emission Factors for Energy Use in Buildings. National Renewable Energy Laboratory, NREL Report TP-550-3861.

Fox, R.W., A.T. McDonald, and P.J. Pritchard, Introduction to fluid mechanics. 6 ed., Hoboken, NJ: John Wiley & Sons, 2004.

Kozubal, E., J. Woods, J. Burch, A. Boranian, and T. Merrigan 2011. Desiccant Enhanced Evaporative Air-Conditioning (DEVap): Evaluation of a New Concept in Ultra Efficient Air Conditioning. National Renewable Energy Laboratory, TP-5500-49722.

Lowenstein, A. 2005. High Efficiency Liquid-Desiccant Regenerator for Air Conditioning and Industrial Drying. AIL Research Inc., Department of Energy Contract No. DE-FG36-03GO13170.

R, 2011. R: A Language and Environment for Statistical Computing. R Development Core Team, Vienna, Austria.

Woods, J. and E. Kozubal 2012. A desiccant-enhanced evaporative air conditioner: Numerical model and experiments. Energ. Convers. Manage., (in review).

Yin, Y.G. and X.S. Zhang 2010. Comparative study on internally heated and adiabatic regenerators in liquid desiccant air conditioning system. Build. Environ., 45(8): p. 1799-1807.